Inorganic Chemistry
Article

A_5InPb_8 (A = K, Rb): An Apparent Zintl Phase with Lead Tetrahedra Interbridged by μ_6-In Atoms[1]

Michael T. Klem and John D. Corbett*

Department of Chemistry and Ames Laboratory−DOE, Iowa State University, Ames Iowa 50011

Reaction of elemental In, Pb, and K, or Rb within welded Ta containers at 900 °C followed by subsequent annealing at 350 °C gives the new phases A_5InPb_8 (A = K, Rb). These crystallize in the trigonal space group $R\bar{3}m$ (No. 166, $Z = 3$) with cell dimensions of $a = 6.8835(6)$ and 6.885(1) Å and $c = 37.591(5)$ and 37.64(2) Å for K_5InPb_8 and Rb_5InPb_8, respectively. The structure contains clusters built of pairs of Pb_4 tetrahedra that are interbridged by a μ_6-In atom. The $InPb_8$ units, which in the isolated case would behave as ideal 40-electron Wade's rule clusters, are weakly interlinked into sheets in the ab plane by long (3.5 Å) intercluster Pb–Pb interactions. According to the EHTB calculations, these cause a broadening of the valence band and thus generate a number of new states at the Fermi level. Compound K_5InPb_8 is metallic ($\rho_{298} \approx 42$ $\mu\Omega$ cm, $(\delta\rho/\delta T)/\rho \approx 1.4(2) \times 10^{-1}$ K^{-1}) which is in agreement with the expectations according to calculations on the anion network.

Introduction

Large deltahedral clusters of group 14 (tetrel, Tt) elements in solid-state systems have been fairly limited. The largest cluster to date is the Tt_9^{4-} anion which is now known for all tetrel elements except for carbon.[2] One of the factors limiting the stability of deltahedral clusters of the heavy tetrel elements is the disproportionate size-to-charge ratio. Wade's rules for counting bonding electron states in a given class of clusters (closo, nido, etc.,) indicate that the charge assigned to an ideal deltahedral tetrel cluster is independent of its nuclearity so that large clusters would carry relatively small negative charges.[3,4] This can presumably set up situations in which the number of cations is insufficient to separate the large clusters, so that cluster fusion or disproportionation occurs, and the cluster compound does not exist. Syntheses in molecular solvents in the past have used large organic

cations or units such as cryptated alkali metal cations to achieve effective separation of clusters.[2,5] In the solid state, larger alkali metal cations, such as Rb and Cs, or cluster substitution with an electron poorer element have been used to circumvent this problem to some degree. It is the latter approach, an attempt to substitute the electron poorer (and smaller) indium atom for lead in the Pb_9^{4-} cluster, that led to the discovery of the electron-richer title compounds, A_8InPb_8, A = K, Rb.

Experimental Section

The materials and general reaction techniques in welded tantalum tubes have been described elsewhere.[6,7] All transfers were completed in a N_2 or He-filled glovebox.

Synthesis. The A_5InPb_8 (A = K, Rb) compounds were obtained by mixing stoichiometric amounts of potassium (Strem, 99.9995%) or rubidium (Strem, 99.999+%) with indium (Aesar, 99.99%) and lead (Aesar, 99.9999%) in tantalum tubes that were then welded shut; the contents were allowed to react at 900 °C and then were annealed at 350 °C for 3 weeks. The results were brittle black crystals. A quantitative yield (>∼95% by powder pattern) of K_5InPb_8 was obtained after the stoichiometry had been established by X-ray crystallography. In most cases, the yield of Rb_5InPb_8 was 80% according to Guinier powder pattern data with the remainder being elemental lead. Attempts to substitute Tl or Ga for In were

(1) This research was supported by the Office of the Basic Energy Sciences, Materials Sciences Division, U.S. Department of Energy (DOE). The Ames Laboratory is operated for the DOE by Iowa State University under Contract No. W-7405-Eng-82.
(2) Queneau, V.; Sevov, S. C. *Angew. Chem., Int. Ed. Engl.* **1997**, *36*, 1754. (b) Schnering, H. G.v.; Baitinger, M.; Bolle, U.; Cabrera, W. C.; Curda, J.; Grin, Y.; Heinemann, L.; Llanos, L.; Peters, K.; Schmeding, A.; Somer, M. *Z. Anorg. Allg. Chem.* **1997**, *623*, 1037. (c) Queneau, V.; Sevov, S. C. *Inorg. Chem.* **1998**, *37*, 1358. (d) Todorov, E.; Sevov, S. C. *Inorg. Chem.* **1998**, *37*, 3889. (e) Queneau, V.; Todorov, E.; Sevov, S. C. *J. Am. Chem. Soc.* **1998**, *120*, 3263.
(3) Wade, K. *Adv. Inorg. Chem. Radiochem.* **1976**, *18*, 1.
(4) Corbett, J. D. In *Chemistry, Structure and Bonding in Zintl Phases and Ions*; Kauzlarich, S., Ed.; VCH: New York, 1996; Chapter 3.
(5) Corbett, J. D. *Chem. Rev.* **1985**, *85*, 383.
(6) Dong, Z.-C.; Corbett, J. D. *J. Am. Chem. Soc.* **1993**, *115*, 11299.
(7) Klem, M. T.; Vaughey, J. T.; Harp, J. G.; Corbett, J. D. *Inorg. Chem.* **2001**, *40*, 7020.

Table 1. Cell Parameters of Trigonal A$_5$InPb$_8$-type Phases (A = K, Rb)[a]

compound	a (Å)	c (Å)	V (Å^3)
K$_5$InPb$_8$	6.8835(6)	37.591(5)	1542.5(5)
Rb$_5$InPb$_8$	6.885(1)	37.64(2)	1543(3)

[a] From Guinier data with Si as an internal standard, 23 °C, and λ = 1.540562 Å.

Table 2. Selected Data Collection and Structural Refinement Parameters for K$_5$InPb$_8$[b]

fw	2959.19
cryst syst, space group, Z[a]	trigonal, $R\bar{3}m$ (No. 166), 3
calcd density (g cm^{-3})	8.508
abs coeff μ(Mo Kα) (cm^{-1})	902.59

[a] Lattice dimensions in Table 1. [b] $R = \sum||F_o| - |F_c||/\sum|F_o|$; $R_w = [\sum w(|F_o| - |F_c|)^2/\sum w(F_o)^2]^{1/2}$; $w = \sigma_F^{-2}$.

unsuccessful as was the attempt to incorporate the larger Cs cation.

X-ray Diffraction. Powder diffraction data obtained with the aid of an Enraf-Nonius Guinier camera and Cu Kα1 radiation were used for phase identification. An improved method for sample mounting for powder pattern measurements was employed. Samples were held between sheets of aluminized polyester film by means of a thin centered film of vacuum grease that also served to seal the outer edge of the sheets and to prevent decomposition of the air sensitive products. This largely avoided a common problem when very sensitive samples of lead compounds are mounted on cellophane tape, the appearance of broad lines of lead in the Guinier powder patterns because of the hydrolysis/oxidation of the mounted sample at room temperature. The films were first compared semiquantitatively with the patterns calculated for phases with known structures. The proportions of the products were then estimated visually from relative powder pattern intensities, considering the unit cell symmetry and contents as well. The cell dimensions of the two new phases as refined from powder data are listed in Table 1.

Several black crystals of K$_5$InPb$_8$ were isolated, sealed into thin-walled capillaries, and checked by Laue photographs. Diffraction data from one specimen were then collected at room temperature using a Rigaku AFC6 diffractometer and monochromated Mo Kα radiation. Routine indexing of 25 centered reflections indicated an R-centered trigonal cell. The absence of other systematic extinctions led to the possible space groups $R\bar{3}m$, $R\bar{3}$, or $R3$. The space group $R\bar{3}m$ was chosen, and this assignment was confirmed by a refinement carried out with the aid of the TEXSAN package.[8] The data were empirically corrected for absorption according to three ψ scans of strong reflections with different θ values. The model was derived by direct methods. The final residuals were $R(F)/R_w$ = 5.7/7.0% with the largest residual in the ΔF map of 3.02 e$^-$/Å^3 located 0.70 Å from K1. The Rb$_5$InPb$_8$ phase was identified via its powder pattern, and lattice parameters were refined using the K$_5$-InPb$_8$ indices as a model.

Selected crystallographic and refinement data are given in Table 2. Refined atom positions are listed in Table 3, and bond distances are listed in Table 4. More detailed information and displacement ellipsoid parameters are given in the Supporting Information, Tables S1 and S2.

Theoretical. Theoretical calculations were made on the full structure over 326 k points in the irreducible wedge with the aid

Table 3. Refined Atomic Positions for K$_5$InPb$_8$ (trigonal setting)[a]

	x	y	z	B_{eq}[b]
Pb1	0	0	0.12864(8)	2.35(4)
Pb2	0.1615(1)	$1 - x$	0.06592(4)	1.42(2)
In	0	0	0	1.19(7)
K1	0	0	0.3180(4)	1.5(2)
K2	0	0	0.2192(5)	2.1(2)
K3	0	0	0.5	4.0(5)

[a] Site symmetries ($R3m$): Pb1 $6c$ $3m$; Pb2 $18h$ $.m$; In $3a$ $\bar{3}m$; K1 $6c$ $3m$; K2 $6c$ $3m$; K3 $3b\bar{3}m$. [b] $B_{eq} = 8/3\pi^2[U_{11}(aa^*)^2 + U_{22}(bb^*)^2 + U_{33}(cc^*)^2 + 2U_{12}(aa^*bb^*)\cos\gamma]$.

Table 4. Atom Separations in K$_5$InPb$_8$ out to 4 Å

atom pair	distance
Pb1−Pb2 ×3	3.045(4)
Pb2−Pb2 ×2	3.337(4)
Pb1−K2 ×3	4.014(4)
Pb1−K2	3.40(2)
Pb1−K3 ×3	4.23(2)
Pb2−In	3.139(2)
Pb2−Pb2[a]	3.551(2)
Pb2−K1 ×3	3.93(1)
Pb2−K1	3.68(2)
Pb2−K2 ×2	3.89(1)
Pb2−K3	4.31(1)
In−K1 ×6	4.018(4)

[a] Intercluster.

of the CAESAR EHTB program produced by Whangbo et al.[9] Only the lead and indium atoms were included because the workable parameters for alkali metal atoms are not available for this method (H$_{ii}$ and ζ_1: for Pb 6s, −15.70 eV and 2.35; for Pb 6p, −8.00 eV and 2.06; for In 5s, −12.60 eV and 1.903; and for In 5p, −6.19 eV and 1.677).[10] Calculations were also carried out on the isolated cluster and a modified version of the full anion substructure in which the individual InPb$_8$ clusters had been separated by over 5 Å in the *ab* plane.

Property Measurements. Resistivities of K$_5$InPb$_8$ were measured by the electrodeless Q method[11] on 44.3 mg that had been sieved to a 250−425 μm powder and diluted with chromatographic Al$_2$O$_3$. Measurements were made at 34 MHz over a range of 120−240 K. The resistivity of K$_5$InPb$_8$ extrapolated to 298 K is 42 $\mu\Omega$ cm with a temperature coefficient [($\delta\rho/\delta T$)/ρ] of 1.4(2) × 10^{-1} K^{-1}. The absolute resistivities may conceivably be in error by a factor of 2 or 3.

Results and Discussion

Description. The basic unit in the structure of K$_5$InPb$_8$ is pairs of Pb tetrahedra that are interbridged by a μ_6-In atom to generate capped and centered InPb$_8$ trigonal antiprisms with the $\bar{3}$ axis along c. The unit cell is shown in Figure 1. The Pb tetrahedra are reasonably somewhat compressed normal to the (Pb2)$_3$ faces with an apex to basal bond distance [(3b-Pb1) − (4b-Pb2)] of 3.045 Å which is 0.292(6) shorter than the corresponding Pb2−Pb2 distances (3.337 Å). The Pb2−Pb2 basal contacts are similarly approximately 0.25 Å longer than the distances found in the tetrahedral Pb clusters in KPb,[12] presumably because of the additional In atom positioned 3.14 Å away between the clusters on a $\bar{3}$

(8) (8) *TEXSAN*, version 1.02 for Windows; Molecular Structure Corp.: The Woodlands, TX, 1997.

(9) Ren, J.; Liang, W.; Whangbo, M.-H. *CAESAR*; PrimeColor Software, Inc.: Raleigh, NC, 1998.

(10) Alvarez, A. Tables of Parameters for Extended Hückel Calculations, Parts 1 and 2, Barcelona, Spain, 1987.

(11) Zhao, J.-T.; Corbett, J. D. *Inorg. Chem.* **1995**, *34*, 378.

between and nearly coplanar with In in three parallel $InPb_8$ clusters where it bonds to three Pb2 atom edges above (3.68 Å) and likewise caps Pb2—Pb2—In faces below (3.93—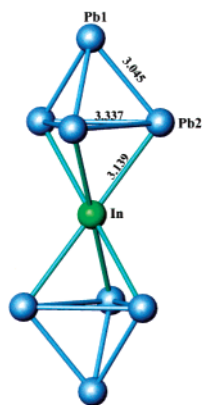4.02 Å) on each (Figure 3a). The K2 cation lies farther away along the 3-fold axis and caps a Pb2—Pb2—Pb1 face (3.89—4.01 Å) on each of three Pb_4 tetrahedra together with being terminal to a Pb1 apex atom (3.40 Å) on a neighboring cluster on the same axis (Figure 3b). The K3 cation lies at a point of $\bar{3}$ symmetry between two layers of $InPb_8$ clusters and bridges six apex—basal (Pb1—Pb2) edges on the ends of six $InPb_8$ clusters, three above and three below, with K3— Pb distances of 4.23 − 4.31 Å (Figure 3c). The first two cations lie in voids with average radii of approximately 3.88 Å while the K3 cations are bound in a cavity with a radius of 4.27 Å. The last represents a void volume increase of approximately 25% and is probably an important factor in the larger size of the K3 ellipsoid.

The occurrences of vertex-fused connections in main group clusters are uncommon. Some examples are known in molecular chemistry with aluminum or silicon as the central atom linking two caps of nido-carboranes in a monocapped square antiprism configuration or pentagonal bypyramids, respectively.[13] Several geometric similarities exist in the solid state as well, for example the mixed alkali metal compounds $A'_7A''E_8$ (E = Ge, Si) in which the smaller A cation occupies a μ_6-capping position between two E_4 tetrahedra (in a staggered configuration).[14,15] Analogous to the role of In here, two examples of group 12 metal-linked tetrel tetrahedra have also been synthesized, Cs_6ZnGe_8 and K_6CdPb_8.[16,17] The former contains isolated clusters isoelectronic with those reported here that are composed of two Ge_4 tetrahedra linked by μ_6-Zn atom in which the Ge_4 tetrahedra are eclipsed, and the latter contains the dimerized equivalent $(Pb_4CdPb_4)Cd(Pb_4$- $CdPb_4)$ (plus isolated Pb_4 tetrahedra) in which interbridged Pb_4 tetrahedra are staggered. The central Cd bridge caps the Pb_3 faces of the two Pb_4CdPb_4. Other known cases of heteroatomically linked tetrahedra of the tetrel elements include $K_4Au(TlSn_3)$[18] and the group $A_3(AuTt_4)$ (A = K, Rb, Cs; Tt = Sn, Pb).[19] These phases contain infinite one-dimensional chains of tetrel tetrahedra that are interbridged on opposed edges by μ_4-Au atoms to form chains.

Bonding. The electronic structure of an isolated $InPb_8{}^{5-}$ cluster can be understood with the aid of extended-Hückel calculations and Wade's rules. According to Wade,[3] the number of skeletal electrons required for closed shell bonding in two tetrahedral nido clusters of lead is $2(2 \times 4 + 4) =$ 24 electrons. Binding these together by a μ_6 bridging indium requires no additional electrons. Each lead atom contributes

Figure 1. ∼[0$\bar{1}$0] view of the structure and trigonal unit cell of the rhombohedral K_5InPb_8 with $\vec{c}$ vertical. Blue, Pb; green, In; yellow, K. Longer intercluster contacts between clusters in the same plane are not marked.

Figure 2. The isolated $InPb_8{}^{5-}$ cluster with the two tetrahedra in a staggered configuration. The green In atom has a $\bar{3}$ local symmetry with the 3-fold axis vertical. (Atoms marked as in Figure 1.)

site. The In1 atom thus links the Pb tetrahedra in an antiprismatic fashion (D_{3d}) (Figure 2).

The cation arrangement about the $InPb_8$ clusters is also of interest as it illustrates well the close anion—cation packing present in this sort of phase. The K1 cation is situated

(12) Hewaidy, I. F.; Busmann, E.; Klemm, W. *Z. Anorg. Allg. Chem.* **1964**, *328*, 283.

(13) (a) Siriwardane, U.; Islam, M. S.; West, T. A.; Hosmane, N. S.; Maguire, J. A.; Cowley, A. H. *J. Am. Chem. Soc.* **1987**, *109*, 4600. (b) Bandman, M. A.; Knobler, C. B.; Hawthorne, M. F. *Inorg. Chem.* **1988**, *27*, 2399.
(14) von Schnering, H. G.; Schwarz, M.; Nesper, R. *Angew. Chem., Int. Ed. Engl.* **1986**, *25*, 566.
(15) Llamos, J.; Nesper, R.; von Schnering, H. G. *Angew. Chem., Int. Ed. Engl.* **1983**, *22*, 998.
(16) Queneau, V.; Sevov, S. C. *J. Am. Chem. Soc.* **1997**, *119*, 8109.
(17) Todorov, E.; Sevov, S. C. *Angew. Chem., Int. Ed.* **1999**, *38*, 1775.
(18) Huang, D.; Corbett, J. D. *Inorg. Chem.* **1998**, *37*, 5007.
(19) Zachwieja, U.; Müller, J. *Z. Anorg. Allg. Chem.* **1998**, *624*, 853.
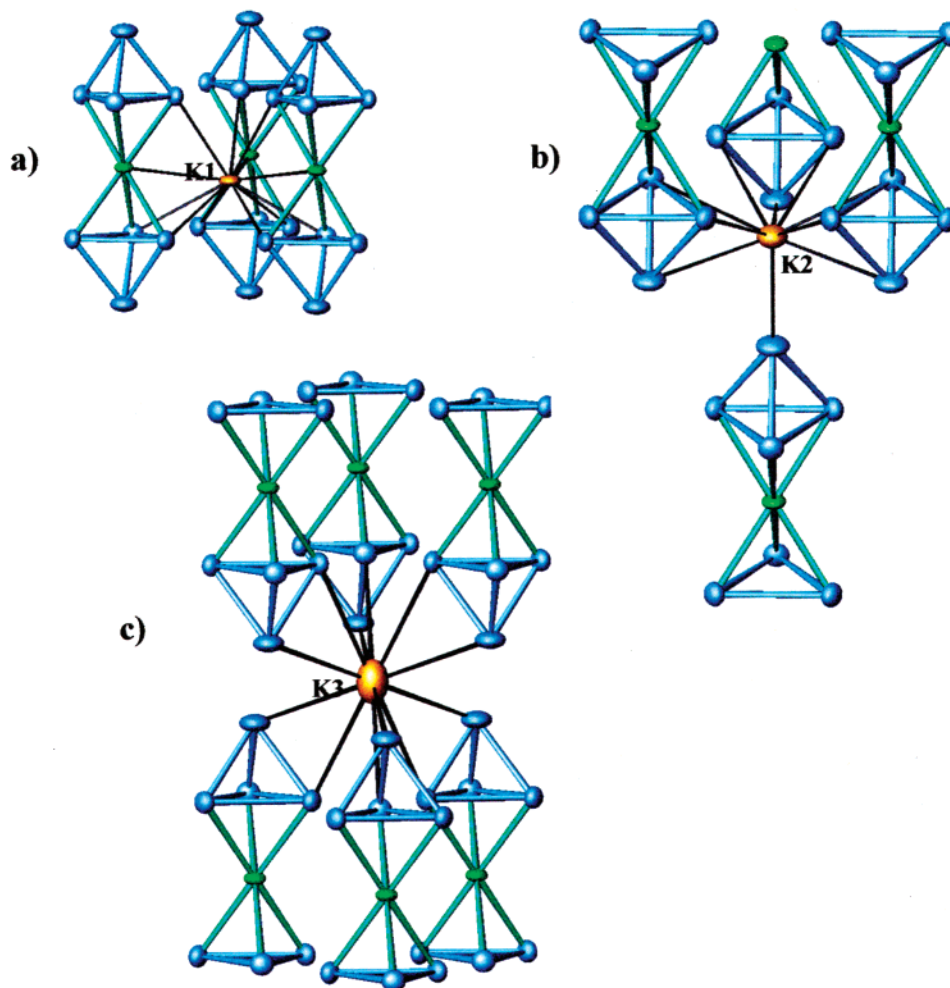
Figure 3. Cation environment in K_5InPb_8 about (a) K1, (b) K2, and (c) K3 (90% probability thermal ellipsoids). K2 and K3 show distortions that originate with their packing environment.

its two valence p electrons, and the indium donates three valence electrons for a total of 19 skeletal electrons. The additional required electrons come from the five alkali metal cations. A molecular orbital calculation for the isolated cluster anion confirms Wade's assignments of 24 electrons for the closed shell cluster (Figure 4). Notwithstanding the expectation of a semiconductor, according to these simple treatments, the measured resistivity of K_5InPb_8 is ~42 $\mu\Omega$ cm at 290 K with a positive temperature coefficient of 0.14 K^{-1}, indicating metallic behavior (Figure 5). In contrast, Cs_6ZnGe_8 with more and larger cations and lighter isoelectronic Ge_8Zn^{6-} oligomers similarly stacked in layers is diamagnetic.[16]

Further considerations suggest two possible explanations for the metallicity. One may be that atoms as heavy as lead do not regularly yield closed shell anions. We have found that this is clearly the case with isolated nominal Pb^{-4} anions with higher field cations in both Ca_5MPb_3 (M = one of several 3d metals) with stuffed Mn_5Si_3Z-type structures[20] and for Ca_3PbO in an inverse perovskite structure when these are analyzed not by EHTB but by relativistic LMTO-ASA

methods.[21] On the other hand, longer intercluster interactions may be sufficient (if not the whole story) according to EHTB methods, as follows.

Further EHTB calculations were carried out on the full structure but again without the cations. The densities-of-states (Figure 6) exhibit a clear separation between the s and p bands of lead with a small contribution from the s and p orbitals of indium. The s contributions from lead dominate up to about -13 eV with a small contribution from indium at ca. -15.5 eV. The DOS plot also reveals a small number of states at the Fermi level with no evidence of a band gap. A broad p band for lead starts at about -12.5 eV and extends past the Fermi level, with only minor In contribution above -8.5 eV. The p_x and p_y orbitals on lead (normal to [001]) are the dominant contributors.

A more critical look at the full structure of A_5InPb_8 aids our understanding of these results. There are multiple moderately long intercluster contacts between coplanar Pb2 atoms in neighboring clusters at distances of 3.54 Å compared with 3.33 Å for the intracluster Pb2−Pb2 bonds. This means the $InPb_8$ clusters are linked via longer Pb2−Pb2 intercluster bonds in the *ab* plane into two-dimensional

(20) Guloy, A. M.; Mudring, A.-V.; Corbett, J. D. *Inorg. Chem.* **2003**, *42*, 6940.

(21) Mudring, A.-V.; Klem, M. T.; Corbett, J. D. Unpublished research.

Figure 4. MO diagram for isolated $InPb_8^{5-}$ cluster (center) and the corresponding fragment orbitals for two Pb_4 tetrahedra (left) and an isolated In atom (right).

Figure 5. Resistivities of K_5InPb_8 according to microwave Q measurements and the least-squares fit. The ρ_{290} extrapolated value is $\sim$42 $\Phi\Omega$ cm.

Figure 6. Densities-of-states and COOP results for the anion network in K_5InPb_8. Orbital components has been projected out in the DOS data, and the COOP data are for the total intracluster (solid) and intercluster Pb−Pb interactions (dotted). The dashed line marks E_F.

Figure 7. [001] view of the layers of $InPb_8$ cluster defined by longer 3.55 Å intercluster Pb−Pb interactions (vs 3.44 Å intracluster separations). Interactions in the layers above and below the (001) plane are marked by light blue and green triangles, respectively.

sheets of clusters. Two of these are shown in Figure 7 in a [001] view, centered around In atoms at $z = 0$ and defined by triangles of Pb2 atoms at opposed ends of the dimer (Figure 2). These 3.54 Å contacts define two nets, above (light blue) and below (blue green) in Figure 7. Each has a significant overlap populations, 0.25 for each of the *intercluster* Pb2−Pb2 (3.54 Å) contacts versus 0.57 and only 0.11 for each *intracluster* Pb1−Pb2 (3.04 Å) and Pb2−Pb2 (3.34 Å) bond. The relatively low overlap population for the intracluster Pb2−Pb2 linkages results, in part, from the occupation of antibonding states by the delocalized electrons (see the COOP data, Figure 6). Further linkage of the sheets of clusters to one another via the apical Pb1 atoms is precluded by their long separation in the *c* direction, 4.90 Å.

That the intercluster contacts are responsible for broadening the valence band is demonstrated by similar calculations

carried out with the clusters separated by 5 Å (Supporting Information). A similar broadening has been found for K_6Pb_8-Cd, a phase that contains $(Pb_4)_4Cd_3$ oligomers (essentially pairs of $InPb_8$-like clusters linked by an additional cadmium atom, plus isolated Pb_4) in which the oligomers likewise have long intercluster Pb−Pb separations, 3.57 Å. Such a calculation on the isolated oligomer also reveals optimization of the bonding within the $CdPb_8^{6-}$ cluster, in accordance with MO and Wade's rules analyses.

With the intercluster bonding in mind, one can begin to understand the reason for having a positive density of states at the Fermi level even though the isolated clusters themselves conform to a Wade's rules assignment. Additional exobonding between neighboring Pb2 atoms effectively oxidizes $InPb_8^{5-}$ to form intercluster bonds, processes that are often thought to involve the lone s pairs. The COOP curves also clearly show that antibonding states within the clusters are being occupied from −7.5 eV up to the Fermi level at −5.6 eV, primarily within the Pb2−Pb2 intracluster bonds. The In−Pb bonding appears to be unimportant around Fermi, but it is a major contributor at lower energies. Interestingly, the intracluster bonding in the extended lattice appears to be optimized at $\sim$6 electrons below that for the isolated cluster, the extra electrons going into the 2D net

shown in Figure 7. The approximations involved in the extended Hückel approach still must not be forgotten. The end result may simply indicate that anionic lead states do not generate a closed shell system and, perhaps, that the supposedly innocent potassium cations, all of which are associated with Pb2 (Figure 3), play a substantial role in delocalized bonding at least around E_F.

Conclusions

The $InPb_8^{5-}$ cluster in the isolated case represents a new Zintl cluster in the heavy tetrel elements, In-bridged pairs of Pb4 tetrahedra. The cluster type is interesting because it is one of the few fused-vertex polyhedra in Zintl chemistry.

The fact that the clusters are not well isolated from one another, probably because of packing effects introduced by the size and relatively low number of cations, leads to a longer range layer structure and metallicity. One can still rationalize the cluster geometry with the observed electron count from a Wade's rules viewpoint.